ACS APPLIED MATERIALS & INTERFACES

Research Article

www.acsami.org

Femtogram Level Detection of Nitrate Ester Explosives via an 8-Pyrenyl-Substituted Fluorene Dimer Bridged by a 1,6-Hexanyl Unit

Lei Chen,[†,‡] Yixun Gao,[†,‡] Yuerong Wang,[†,‡] Chao He,[†] Defeng Zhu,[†] Qingguo He,*,[†] Huimin Cao,[†] and Jiangong Cheng*,[†]

[†]State Key Lab of Transducer Technology, Shanghai Institute of Microsystem and Information Technology, Chinese Academy of Sciences, 865 Changning Road, Shanghai 200050, China

[‡]University of Chinese Academy of Sciences, 19 Yuquan Road, Beijing 100039, China

Supporting Information

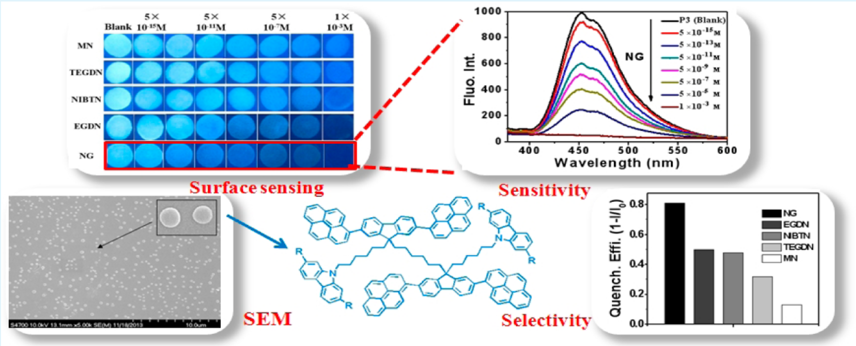

ABSTRACT: Compared with nitroaromatic explosives detection, nitrate esters are far from wide attention possibly because of their shortage of aromatic ring and difficulty in being detected. Three fluorescent chemical probes for trace nitrate ester detection: an intramolecular dimer (**P3**) of 8-pyrenyl-substituted fluorenes bridged by a 1,6-hexanyl unit as well as its counterparts 2PR-F (**P1**) and 2PR-Cz (**P2**) has been synthesized and characterized. Their chemical structures and photophysical and electrochemical properties show that the dimer **P3** film has a higher molar extinction coefficient, larger steric hindrance, higher area-to-volume ratio, and matching energy level with nitrate ester explosives, which contributes to higher sensitivity and moderate selectivity for sensing of nitrate ester explosives such as nitroglycerin (NG). The fluorescence of the **P3** film is rapidly about 90% quenched upon exposure to a saturated vapor of NG for 50 s and almost 100% quenched for 300 s at room temperature due to photoinduced electron transfer between the probe and analyte. In addition, a very sensitive, rapid, simple, and low-cost surface-sensing method by disposable filter-paper-based test strips is demonstrated. The contact-mode approach exhibits a detection limit as low as 0.5 fg/cm^2 for NG. These results reveal that the multiple-pyrenyl-unit-substituted fluorene dimer **P3** is suitable for preparing a highly sensitive and efficient thin-film device for detecting nitrate esters.

KEYWORDS: *fluorescent probe, femtogram, nitroglycerin, fluorescence quenching, surface sensing*

1. INTRODUCTION

In recent years, with the development of social unrest in some areas, ethnic conflicts and terrorism,[1] accurate and reliable detection of trace explosives has become a focal point at the airport, subway, and other public places as well as military battlefield. More and more scientists from different fields are striving to solve this problem. Currently, detection technologies of trace explosives include gas chromatography−mass spectrometry,[2] gas chromatography with electron capture,[3] surface-enhanced Raman spectroscopy,[4] mass spectrometry,[5] X-ray imaging,[6] electrochemical methods,[7] ion migration spectrometry,[8] etc. These methods have certain advantages and adaptability to analyze suspicious materials, but there are some shortcomings and negative factors such as a cumbersome analysis process, expensive and complicated equipment, serious interference, and robust portability. Thus, a great demand for a sensitive, selective, and rapid on-site explosives detection method remains.

Electron-deficient nitro aromatic explosives such as TNT, DNT, and PA can easily interact with an electron-rich chromophore by intermolecular $\pi-\pi$ stacking, resulting in photoinduced electron transfer (PET) between them, which is the basis for explosives detection. Most reported[9−14] sensory materials for explosives detection are fluorescent conjugated polymers such as PPE and PPV utilizing the molecular wire effect to afford very high sensitivity. Compared with nitro aromatics, nitrate esters such as nitroglycerin (NG) and ethylene glycol dinitrate (EGDN) with O−NO$_2$ moieties are

Received: March 18, 2014
Accepted: April 22, 2014
Published: April 22, 2014

dx.doi.org/10.1021/am501543f | *ACS Appl. Mater. Interfaces* 2014, 6, 8817−8823

aliphatic explosives, as shown in Figure 1a. Owing to a shortage of conjugated aromatic rings, nitrate esters cannot interact with the fluorescent probe by intermolecular π–π stacking, which makes their optical detection challenging.[15,16] On the other hand, nitrate esters have relatively low saturated vapor pressure (e.g., the saturated vapor pressure of NG at room temperature is only about 0.5 ppm). Therefore, efficient detections of nitrate esters based on the fluorescent method are less reported. Recently, most reports on nitrate ester detection are based on some expensive and complicated equipment. For example, Waldemar et al. reported that the detection limit of NG is as low as 100 ng with an ion-mobility spectrometry vapor detector and operated in particle mode.[17] McCord et al. reported a detection limit of 64 ng for NG by an ultraperformance liquid chromatography with tandem mass spectrometry method.[18] Nevertheless, fluorescence sensing technology will be highly favored for nitrate ester detection because of its high sensitivity, high specificity, fast response, low cost, lack of sample processing, and antienvironmental interference ability. For efficient detection of nitrate esters, new sensing materials with high performance should be developed.[19−21]

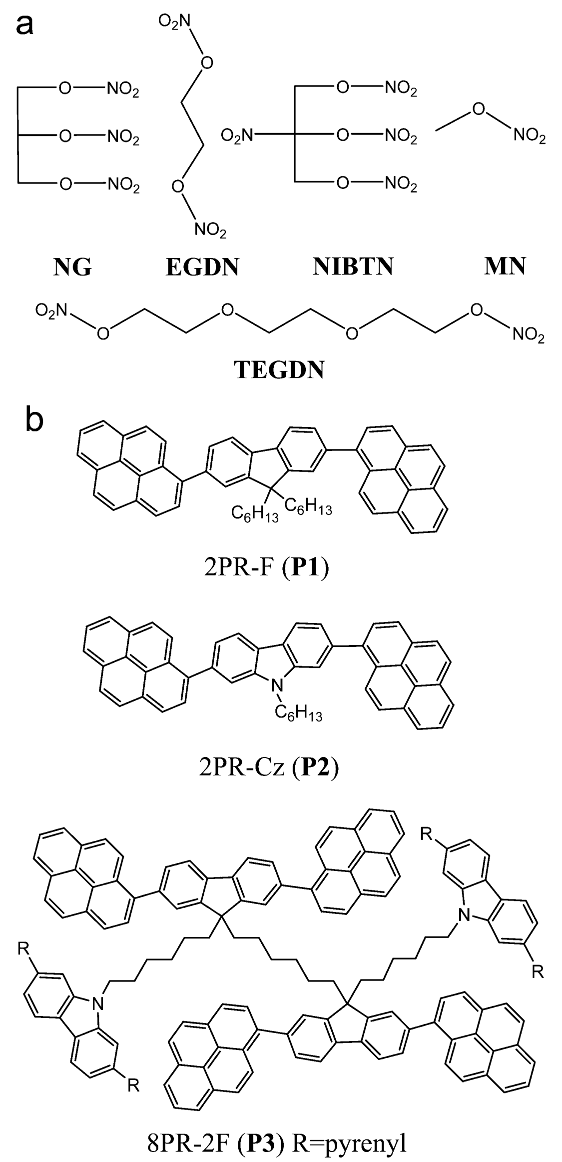

Figure 1. (a) Chemical structures of the nitrate ester explosives cited in this paper. (b) Chemical structures of **P1**−**P3**.

Compared with conjugated polymers, organic conjugated materials of small molecules have obvious advantages in purification and characterization, structure control, solubility, and tunable luminescence properties.[22] However, generally, the sensitivity of the polymer is much higher than that of the corresponding small molecule because of the molecular wire effect of the polymer, while if the small-molecule material could be highly fluorescent and bear a suitable energy level and if its aggregation state could be well controlled to afford a high area-to-volume ratio for efficient analyte permeability, it is entirely possible to improve the sensing performance.[23] Explosive-detecting materials like metal−organic frameworks (MOFs), which have high area-to-volume ratios, are excellent candidates for sensing.[24] Nagarkar et al. reported a 3D fluorescent MOF for the highly selective detection of the nitro explosive TNP in solution.[25] It shows a new route to designing sensing probes with high specific surface area for high sensing performance.

Previously, an 8-pyrenyl-substituted fluorene dimer bridged by a 1,6-hexanyl unit (**P3**) and its counterparts 2PR-F (**P1**) and 2PR-Cz (**P2**) (Figure 1b) has been synthesized and reported in our laboratory,[26] which is proven to be a simple and effective way to prepare amorphous fluorene derivatives. However, subsequent tests with **P3** as an electroluminescent material are proven to be not efficient because **P3** tends to be assembled into a nanosphere-composed coarse film rather than a smooth and pinhole-free film.

In spite of this, a nanosphere-composed coarse film means that the film will have a high area-to-volume ratio for efficient analyte permeability, which will be highly favorable for sensing applications. Reported herein is that **P3** is adopted as a probe to explore its sensing performance for nitrate ester explosives such as NG by a PET-induced fluorescence quenching method considering its high molar extinction coefficient, high quantum yield, and high area-to-volume ratio. As expected, the dimer 8PR-2F (**P3**) can act as a fluorescence "turn-off" probe for nitrate ester explosives and shows significant quenching of fluorescence in the presence of NG compared to other different nitrate esters. In addition, surface detection for nitrate ester explosives based on **P3** filter-paper strips is developed. A visual detection limit down to the femtogram level is remarkably achieved, which is a rapid, simple, and low-cost method for the detection of NG on the surface.

2. EXPERIMENTAL SECTION

2.1. Instruments and Materials. UV−vis absorption and fluorescence analysis were obtained from a Jasco V-670 spectrophotometer and a Jasco FP 6500 spectrometer, respectively. Cyclic voltammetry (CV) experiments were performed with a CH Instruments electrochemical analyzer. The electrochemical behaviors of **P1**−**P3** as well as the nitrate esters were investigated in a standard three-electrode electrochemical cell (a glassy carbon working electrode, a platinum counter electrode, and a saturated calomel electrode as the reference electrode) with 0.1 M tetra-*n*-butylammonium hexafluorophosphate (Bu_4NPF_6) in an acetonitrile solution, and the scanning rate was 100 mV/s under a nitrogen atmosphere at room temperature.

Previously, **P1**−**P3** have been synthesized and reported in our laboratory. All solvents and reagents were obtained from commercial sources and used as received. The sensing films were prepared by dip-coating toluene solutions (10^{-4} M) of **P1**−**P3** onto a piece of 10 × 20 mm quartz plate and vacuum-dried for half an hour before use. The fluorescence responses of films to diverse nitrate esters were progressed by inserting the films into hermetically sealed vials (3.8 mL) containing cotton and analyte at room temperature, which could prevent direct contact between the probe and analyte as well as help to maintain a constant vapor pressure. The fluorescent time-course responses were recorded as soon as the film was exposed to analyte vapor and ended at 300 s.

2.2. Surface-Sensing Experiment. In order to explore the detection limit of **P3** for nitrate esters by contact mode, we carried out a surface-sensing approach by using a glass microsyringe to drop a 3 μL toluene solution of **P3** (10^{-4} M) onto the filter paper, which produced a fluorescent spot with less than 1 cm diameter (approximately 0.8 cm^2 area of a spot) followed by drying under a hair dryer and cutting of the dried filter paper into pieces. Different concentrations of nitrate ester solutions (5×10^{-15}–1×10^{-3} M) were prepared by serial dilutions in acetone. The explosive solutions prepared from a 5 μL volume were spotted onto fluorescent spots of **P3** on filter paper, and a solvent blank of pure acetone was used as a control test. In order to control the consistency of the test angle, the filter-paper piece was clamped with a clip at an angle of 45° to the incident light to scan the emission spectra by a Jasco FP 6500 spectrometer.

3. RESULT AND DISCUSSION

3.1. Optical and Electrochemical Properties. Figure 2 shows the absorption and emission spectra of **P1**–**P3** films prepared from their toluene solutions with a concentration of 10^{-4} M. The optical absorption and emission results of both in solution and as a dip-coated film are summarized in Table 1 and Figure S1 (Supporting Information, SI). It could be found that the absorption and fluorescence maxima of all three probes experience a red shift from solution to the film state. The absorption peaks of the **P1** and **P2** films are red-shifted by 22 and 16 nm, while that of the **P3** film is only red-shifted by 12 nm. Similarly, the emission peak of the **P3** film shows a red shift of 27 nm relative to 34 nm for the **P1** film, which even has a very wide emission peak. These results indicate that there is larger steric hindrance in the dimer structure of **P3**, which is beneficial for preventing the resulting π–π-stacking self-aggregation effect in the solid state and hence favorable for improving the fluorescent intensity and sensitivity of the probe.

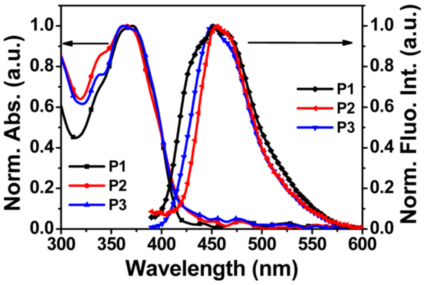

Figure 2. UV–vis absorption and emission spectra of **P1**–**P3** films.

As shown in Table 1 and Figure S1 in the SI, molar extinction coefficients (ε_{max}, determined in their toluene dilute solution) of the three probes increase sharply with the number of pyrene groups of the molecules. There are nearly 1.8- and 2.4-fold increases from that of **P1** (log ε_{max} = 5.00) to **P2** (log ε_{max} = 4.92) to **P3** (log ε_{max} = 5.45). A high molar extinction coefficient is very critical for detection instruments based on optical response because of the more efficient harvesting of the excitation energy so that the dimer **P3** is more suitable for the photoresponsive devices as more sensitive materials compared with the monomers. In addition, the fluorescent quantum yield (Φ) is also an important factor for sensing materials. As presented in Table 1, all three probes demonstrate very high Φ in their tetrahydrofuran (THF) solution, especially for **P3** and **P1**, which are nearly 1. Higher efficient light emission, combined with larger steric hindrance and higher light absorption capacity, suggests that **P3** is likely a promising candidate for sensing application.

The energy-level matching between the probe and analyte is crucial for the sensing process based on a PET sensing mechanism. We previously tested and reported the CV curves of **P1**–**P3** and calculated their highest occupied molecular orbital (HOMO) and lowest unoccupied molecular orbital (LUMO) levels.[26] Corresponding data are summarized in Table 1. The LUMO levels of the monomers **P1** and **P2** and dimer **P3** are all higher than those of the nitrate esters discussed here. Also, the energy gap (ΔE) of **P3** is 3.04 eV compared with 3.19 and 3.15 eV for **P1** and **P2**, respectively, which implies that a longer-wavelength light source will be needed for excitation. It is also important for the construction of a low-price detector and reduces photooxidation of the sensory material from the light source.

3.2. Detection of Nitrate Esters in the Vapor Phase. This study is intended to detect nitrate ester vapor such as NG by a fluorescent quenching sensing method. The LUMO level of NG is −3.39 eV, which is lower than those of **P1**–**P3**. Thus, the prerequisite for PET (**P3** as an example) is satisfied, as shown in Figure 3. Namely, nitrate esters such as NG can act as electron acceptors, and fluorescence is likely quenched by the analyte via a PET mechanism.[27,28]

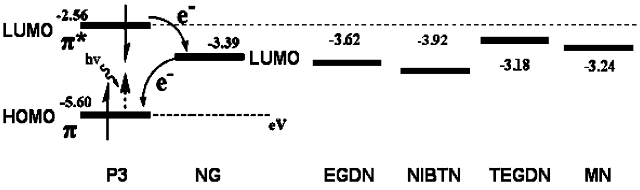

Figure 3. PET process of fluorescence quenching.

Figure 4 first shows that the photobleaching extent of the probes is less than 3% within 300 s in the air conditions at room temperature (25 °C). This demonstrates that the photostability of **P1**–**P3** is excellent. Then, sensing perform-

Table 1. Optical and Electrochemical Properties of P1–P3

	abs, λ_{max} (nm)		PL, λ_{max} (nm)						
	solution	film	solution	film	HOMO (eV)	LUMO (eV)	ΔE (eV)	Φ^a	log ε_{max}^b
P1	349	371	419	453	−5.93	−2.74	3.19	1	5.00
P2	348	364	431	456	−5.81	−2.66	3.15	0.82	4.92
P3	350	362	425	452	−5.60	−2.56	3.04	0.97	5.45

[a] The fluorescence quantum yields of **P1**–**P3** compounds in a THF dilute solution were measured using a dilute solution of 9,10-diphenylanthracene ($\Phi \sim 1$) in a THF solution as the standard. [b] The molar absorption coefficient was measured at the absorption maximum (λ_{max}).

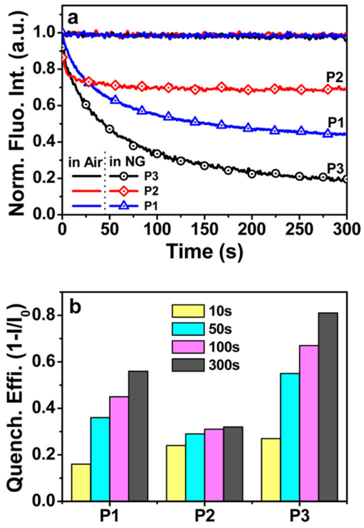

Figure 4. (a) Stability and sensing properties of **P1**−**P3** films exposed to air and saturated NG vapor respectively within 300s. (b) Quenching efficiency of **P1**, **P2**, and **P3** films at different times in saturated NG vapor.

ance analysis shows that the dimer **P3** film produces rapid and significant fluorescence quenching with a response rate of about 27% within 10 s and about 55% within 50 s upon exposure to saturated NG vapor. The final quenching efficiency is about 81% within 300 s, which is far better than that of **P1** and **P2**, whatever the instant quenching rate or lifetime of the device (56% and 32% quenching efficiency within 300 s for **P1** and **P2**, respectively).

We ascribe the sensing difference to the different molecular structures of the probes. The hexanyl unit within dimer **P3** is used as a bridge to connect two fluorene moieties in order to adjust the distance between the chromophores, which produces very high steric hindrance and is also responsible for the nanosphere morphology formation due to intermolecular assembly during the dip-coating process. Under the same conditions, monomers **P1** and **P2** have no such similar self-organization ability. Scanning electron microscopy (SEM) shows that only uniform and smooth films are formed for **P1** and **P2**, as shown in Figure S3 (SI). High steric hindrance of the **P3** film can suppress the intermolecular $\pi-\pi$-interaction-induced fluorescence quenching and increase the vapor permeability. Meanwhile, amorphous spheres can provide larger contact area to capture more analyte molecules and trigger larger signal change. In addition, the high molar extinction coefficient, the high fluorescence intensity, and the relatively low band gap of **P3** are conducive to triggering a large optical signal change under low-power light source excitation.

To further optimize the sensing performance of **P3**, the thickness of the dip-coating film was tuned via a concentration control from 10^{-3} to 10^{-5} M. It is found that a concentration of 10^{-4} M is the most ideal for film fabrication compared with the concentrations of 10^{-3} and 10^{-5} M, which showed the best sensing performance for NG, as shown in Figure S4 (SI). The result indicates that the thickness of the sensing film, that is to say, the appropriate concentration of the probe, should be considered for better vapor penetration and contact with the analyte. On the other hand, the solvent effect on the surface morphology of the sensing film related to the sensing performance change was explored. **P3** was dissolved in toluene, THF, and methylene chloride (all with a concentration of 10^{-4} M) respectively, followed by the preparation of sensing films under the same dip-coating condition. Figure 5 shows

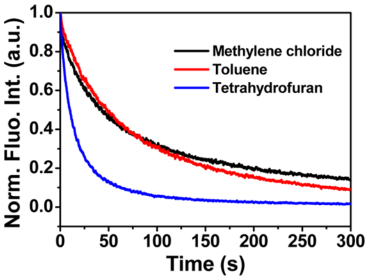

Figure 5. Sensing properties of **P3** films prepared with different solvents exposed to saturated NG vapor.

approximately 90%, 100%, and 85% fluorescent quenching for the films prepared from toluene, THF, and methylene chloride solutions, respectively. The film prepared from a THF solution clearly shows the most significant and rapid fluorescent quenching (90% within 50 s and 100% within 300 s) upon exposure to NG vapor. To interpret the solvent effect on the film morphology, Figure 6 reveals SEM images of **P3** films prepared with different solvents. As can be seen, the **P3** film prepared with THF shows a morphology of more dense and smaller nanoparticles, resulting in a larger area-to-volume ratio than that prepared with toluene. However, the film from methylene chloride only demonstrates quite different and heavy aggregation, and no such nanoparticles could be found.

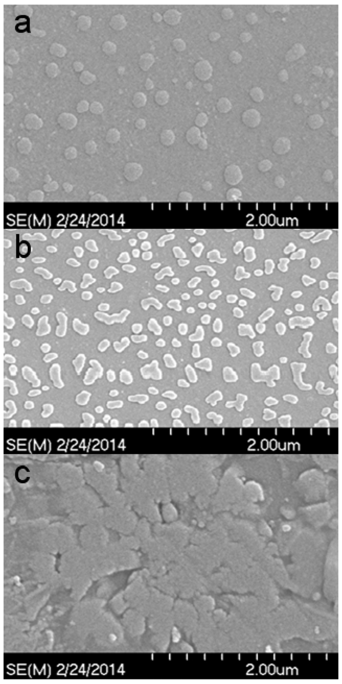

Figure 6. SEM images of **P3** films prepared with toluene (a), THF (b), and methylene chloride (c) solvents (all with a concentration of 10^{-4} M).

The selectivity is another important issue for the sensing behavior. The sensing response of the **P3** film upon exposure to saturated vapor of different nitrate ester explosives is shown in Figure 7. Concerning data of the saturated vapor pressure and LUMO levels of nitrate esters are also illustrated in Table 2. At

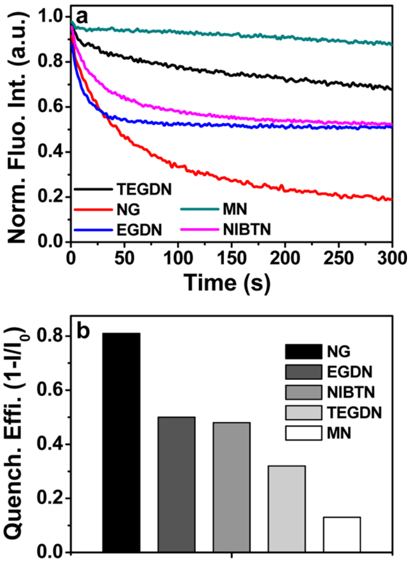

Figure 7. (a) Sensing properties of the **P3** film exposed to different nitrate ester saturated vapors respectively within 300 s. (b) Quenching efficiency of the **P3** film to different nitrate ester saturated vapors after an exposure of 300 s.

Table 2. Saturated Vapor Pressure and LUMO Level of Different Nitrate Esters

	NG[a]	MN[a]	EGDN[b]	TEGDN[c]	NIBTN[d]
V_p/ppm (25 °C)	0.49	1355	36.8	<1.38	<NG
LUMO[e] (eV)	-3.39	-3.24	-3.62	-3.18	-3.92

[a] *CRC Handbook on Vapor Pressure*. [b] Sanchez, J. C.; Trogler, W. C. *J. Mater. Chem.* **2008**, *18*, 3143−3156. [c] Ou, Y. X. Explosives Science; Beijing Institute of Technology Press: 2006. [d] Meyer, R. Köhler, J.Homburg, A. *Explosives* **2007**, 230−231. [e] Calculated from CV experiments, as shown in Figure S2 (SI).

room temperature, the **P3** film produces a rapid, significant fluorescent quenching response within 300 s to NG (~81% quenching), EGDN (~50%), and nitroisobutyl trinitrate (NIBTN, ~50%), while other nitrate esters such as methyl nitrate (MN, ~10%) and triethylene glycol dinitrate (TEGDN, ~30%) show lower quenching efficiencies (Figure 7b). In addition, other commonly used solvent vapors were also tested, and none of them interfere with the sensing process to NG vapor, as shown in Figure S5 (SI).

To interpret the sensing performance on the selectivity, three factors should be considered, namely, the relative LUMO level position, interaction force between the probe and analyte, and the saturated vapor pressure of the analyte. The LUMO level of **P3** is higher than that of all of these nitrate esters to ensure the occurrence of PET, which is the thermodynamic basis. However, NG exhibits the highest quenching efficiency, EGDN and NIBTN shows a moderate response, and the least efficient are MN and TEGDN. The results indicate that PET is not the decisive factor for fluorescence quenching.[28] The saturated vapor pressure is also an important factor in generating fluorescence quenching of the probe. The sensing responses of TEGDN and NIBTN are not ideal possibly because of their low saturated vapor pressure (Table 2). In comparison, EGDN can be rapidly and reliably detected in 42% quenching efficiency within 25 s because of its relatively high saturated vapor pressure.[29] In addition, compared with the vapor pressure, the interaction force seems to be a more important factor. The dynamical process will be determined by the interaction force between the quencher and molecular probe including dipole−dipole interaction, hydrogen-bonding interaction, hydrophobic−hydrophobic interaction, etc. As for NG and MN, although MN has a higher vapor pressure (1355 ppm) than NG (0.49 ppm), NG bears three nitro units, while MN has only one so that the interaction force between NG and **P3** including dipole−dipole interaction and hydrogen bonding interaction is possibly much stronger than that of MN, which makes the quenching efficiency of NG far better than that of MN. Thus, in the PET quenching mechanism of nitrate ester detection, both the electron-donating ability of the probe and the electron-accepting ability of the quencher have a great influence on the sensing response.

3.3. Detection Limit of Nitrate Esters in Surface Sensing. Contact-mode inspection is appropriate for the chemical residual contamination detection of explosives.[30] In order to explore the detection limit of **P3** for NG by contact mode, we carried out a surface-sensing approach. Upon contact with NG, the blue luminescence of **P3** (3 μL) began to fade (after 20 s exposure to UV light) to a dark spot (approximately 0.8 cm^2 area) for NG. The visual fluorescence quenching efficiency was found to decrease with reduction of the NG concentration levels and the limit of NG detectable by the naked eye is as low as 5×10^{-13} M under irradiation with 365 nm UV light. The same experiment was expanded to other nitrate esters including EGDN, MN, NIBTN, and TEGDN, as shown in Figure 8c.

Figure 8a shows the change of the emission spectra of **P3**-dropped filter paper against different concentrations of NG solutions (5×10^{-15}−1×10^{-3} M) at room temperature. The fluorescence quenching efficiency decreases with a decrease in the concentration of NG. 8% and 22% quenching are observed for 5×10^{-15} and 5×10^{-13} M solutions of NG, respectively. The detectable minimum amount of NG by the naked eye is as low as a 5×10^{-13} M (1.135×10^{-13} g/mL) solution with a remarkable detection limit of about 0.5 fg/cm^2. Meanwhile, quenching efficiencies of various nitrate esters toward the fluorescence of **P3**-dropped filter paper are shown in Figure 8b. Consistent with the results of previous vapor detection, the quenching efficiency of the NG solution is more obvious than those of other types of nitrate ester explosives. Because of rapid evaporation,[28] EGDN can only be detected at a 30 fg/cm^2 level. Fluorescent spots maintain their bright-blue luminescence for MN, TEGDN, and NIBTN, resulting in a much poorer level detection as observed. In short, filter paper represents a kind of semiporous material typically used for penetration of the analyte so that it facilitates full access of the analyte with the probe, and as the substrate, it will be highly efficient for improving the detection limit in current technology.[31] The detection ability of **P3** for these explosives can satisfy the on-site, sensitive, simple, rapid, and low-cost request[32] for the field detection of NG on a surface as demonstrated.

4. CONCLUSION

In conclusion, a very sensitive, rapid, simple, and low-cost vapor-phase and surface-sensing method based on a fluorescent chemical probe, 8-pyrenyl-substituted fluorene intramolecular dimer (**P3**) for trace nitrate ester explosives detection is reported. As a fluorescent probe for NG vapor, the dimer **P3** shows more rapid and significant fluorescence quenching and moderate selectivity mainly because of its higher molar extinction coefficient, larger steric hindrance, higher area-to-

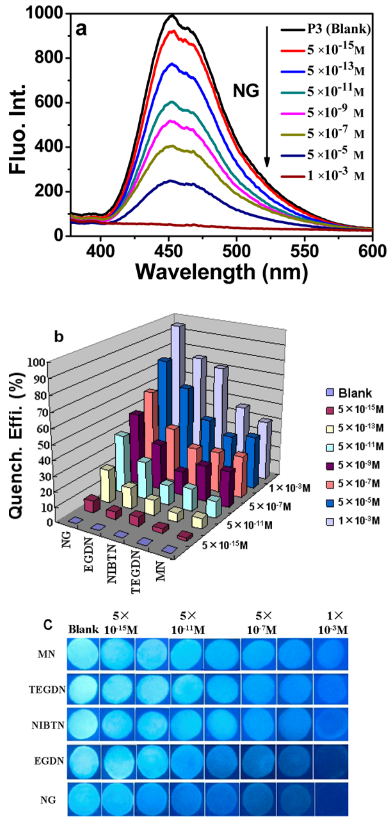

Figure 8. (a) Change in the emission spectral pattern of **P3**-dropped filter paper against different concentrations of NG solutions (5×10^{-15}–1×10^{-3} M) and a solvent blank of pure acetone as a control. (b) Quenching efficiency of various nitrate esters toward the fluorescence emission of **P3**-dropped filter paper. (c) Photograph of **P3**-dropped filter paper before and after the addition of different concentrations of various nitrate esters under a UV lamp at 365 nm by the contact-mode method.

volume ratio, and matching energy level with nitrate ester explosives compared with its monomer counterparts **P1** and **P2**. In addition, the sensing property of **P3** is significantly influenced by the state of the sensitive thin films such as thickness, morphology, and binding capacity between the probe and analyte. Last but not least, a surface-sensing method by disposable filter-paper-based test strips is successfully demonstrated for a range of nitrate esters including NG, EGDN, TEGDN, NIBTN, and MN. The detection limit for NG in the contact mode is achieved to be as low as the femtogram level (0.5 fg/cm^2). This method provides a new route for the trace and on-site detection of nitrate ester explosives, which has great relevance to human health, public safety, and national defense.

■ ASSOCIATED CONTENT

Ⓢ Supporting Information

Information on the supplementary spectra, CV curves, SEM images, and part of the sensing performance of the materials for nitrate ester explosives detection in the vapor phase and surface sensing. This material is available free of charge via the Internet at http://pubs.acs.org.

■ AUTHOR INFORMATION

Corresponding Authors

*E-mail: hqg@mail.sim.ac.cn.
*E-mail: jgcheng@mail.sim.ac.cn.

Notes

The authors declare no competing financial interest.

■ ACKNOWLEDGMENTS

We thank the research programs from the National Natural Science Foundation of China (Grants 61325001, 21273267, and 51272191), Ministry of Science and Technology of China (Program 2012BAK06B03), and Shanghai Science and Technology Committee (Grant 11JC1414700).

■ REFERENCES

(1) Rouhi, A. M. Land Mines: Horrors Begging for Solutions. *Chem. Eng. News.* **1997**, *75*, 14–22.

(2) Kristina, H.; Ramal, V. C.; Roman, A. Z.; Victor, L. T.; Per, H. Low-mass Ions Observed in Plasma Desorption Mass Spectrometry of High Explosives. *J. Mass Spectrom.* **2000**, *35*, 337–346.

(3) Walsh, M. E. Determination of Nitroaromatic, Nitramine, and Nitrate Ester Explosives in Soil by Gas Chromatography and an Electron Capture Detector. *Talanta* **2001**, *54*, 427–438.

(4) James, M. S.; James, A. J.; Klein, J. D.; Kevin, M. S. Surface-enhanced Raman Detection of 2,4-Dinitrotoluene Impurity Vapor as a Marker to Locate Landmines. *Anal. Chem.* **2000**, *72*, 5834–5840.

(5) Mathurin, J. C.; Faye, T.; Brunet, A.; Tabet, J. C. High Pressure Ion Source Combined with an In-Axis Ion Trap Mass Spectrometer. 1. Instrumentation and Applications. *Anal. Chem.* **2000**, *72*, 5055–5062.

(6) Susan, F. H. Screening People for Illicit Substances: a Survey of Current Portal Technology. *Talanta* **2001**, *54*, 447–458.

(7) Krausa, M.; Schorb, K. Trace Detection of 2,4,6-Trinitrotoluene in the Gaseous Phase by Cyclic Voltammetry. *J. Electroanal. Chem.* **1999**, *461*, 10–13.

(8) Eiceman, G. A.; Stone, J. A. Ion Mobility Spectrometers in National Defense. *Anal. Chem.* **2004**, *76*, 390A–397A.

(9) Jichang, F.; Yang, L.; Mujie, Y. Conjugated Polymer-Grafted Silica Nanoparticles for the Sensitive Detection of TNT. *Sens. Actuators, B* **2010**, *145*, 438–443.

(10) Taihong, L.; Liping, D.; Keru, Z.; Wenliang, W.; Yu, F. Single-Layer Assembly of Pyrene End-Capped Terthiophene and its Sensing Performances to Nitroaromatic Explosives. *J. Mater. Chem.* **2012**, *22*, 1069–1077.

(11) Jennifer, L. N.; William, R. D. Conjugated Porous Polymers for TNT Vapor Detection. *ACS Macro Lett.* **2013**, *2*, 423–426.

(12) Andrew, T. L.; Swager, T. M. Detection of Explosives via Photolytic Cleavage of Nitroesters and Nitramines. *J. Org. Chem.* **2011**, *76*, 2976–2993.

(13) Deng, C.; Gong, P.; He, Q.; Cheng, J.; He, C.; Shi, L.; Zhu, D.; Lin, T. Highly Fluorescent TPA-PBPV Nanofibers with Amplified Sensory Response to TNT. *Chem. Phys. Lett.* **2009**, *483*, 219–223.

(14) Samuel, W. T.; G.uy, D. J.; Timothy, M. S. Chemical Sensors Based on Amplifying Fluorescent Conjugated Polymers. *Chem. Rev.* **2007**, *107*, 1339–1386.

(15) Yolanda, S.; Romón, M. M.; María, D. M.; Félix, S.; Ana, M. C.; Margarita, P.; Salvador, G. Optical Chemosensors and Reagents to Detect Explosives. *Chem. Soc. Rev.* **2012**, *41*, 1261–1296.

(16) Ying, W.; Anthony, L.; Yu, D.; Yixin, L.; Yu, L. Novel Signal-Amplifying Fluorescent Nanofibers for Naked-Eye-Based Ultrasensitive Detection of Buried Explosives and Explosive Vapors. *Adv. Funct. Mater.* **2012**, *22*, 3547–3555.

(17) Anna, Z.; Wojciech, P.; Waldemar, T. Limits of Detection of Explosives as Determined with IMS and Field Asymmetric IMS Vapour Detectors. *Forensic Sci. Int.* **2013**, *226*, 168–172.

(18) Jennifer, L. T.; Danielle, L.; Bruce, R. M. Separation and Detection of Smokeless Powder Additives by Ultra Performance Liquid Chromatography with Tandem Mass Spectrometry (UPLC/MS/MS). *J. Forensic Sci.* **2013**, *58*, 609–615.

(19) Stringer, R. C.; Gangopadhyay, S.; Grant, S. A. Detection of Nitroaromatic Explosives Using a Fluorescent-Labeled Imprinted Polymer. *Anal. Chem.* **2010**, *82*, 4015–4019.

(20) Miao, X.; Benjamin, R. B.; Ling, Z. Paper-Based Vapor Detection of Hydrogen Peroxide: Colorimetric Sensing with Tunable Interface ACS. *ACS Appl. Mater. Interfaces* **2011**, *3*, 642−647.

(21) Gardner, J. W.; Yinon, J. *Electronic Noses & Sensors for the Detection of Explosives*; Kluwer Academic Publishers: Dordrecht, The Netherlands, 2004.

(22) Zhankuai, P.; Silu, T.; Xiaohong, Z.; Jianxin, T.; Chunsing, L.; Shuittong, L. New Fluorene Derivatives for Blue Electroluminescent Devices: Influence of Substituents on Thermal Properties, Photoluminescence, and Electroluminescence. *J. Phys. Chem. C* **2008**, *112*, 2165−2169.

(23) Liping, D.; Yu, F. Chemically Assembled Monolayers of Fluorophores as Chemical Sensing Materials. *Chem. Soc. Rev.* **2010**, *39*, 4258−4273.

(24) Stylianou, K. C.; Heck, R.; Chong, S. Y.; Bacsa, J.; Jones, J. T. A.; Khimyak, Y. Z.; Bradshaw, D.; Rosseinsky, M. J. A Guest-Responsive Fluorescent 3D Microporous Metal−Organic Framework Derived from a Long-Lifetime Pyrene Core. *J. Am. Chem. Soc.* **2010**, *132*, 4119−4130.

(25) Nagarkar, S. S.; Joarder, B.; Chaudhari, A. K.; Mukherjee, S.; Ghosh, S. K. Highly Selective Detection of Nitro Explosives by a Luminescent Metal−Organic Framework. *Angew. Chem., Int. Ed.* **2013**, *52*, 2881−2885.

(26) Chao, H.; Qingguo, H.; Qing, C.; Liqi, S.; Huimin, C.; Jiangong, C.; Changmin, D.; Tong, L. Highly Fluorescent Intramolecular Dimers of Two Pyrenyl-Substituted Fluorenes Bridged by 1,6-Hexanyl: Synthesis, Spectroscopic, and Self-Organized Properties. *Tetrahedron Lett.* **2010**, *51*, 1317−1321.

(27) Jiasheng, W.; Weimin, L.; Jiechao, G.; Hongyan, Z.; Pengfei, W. New Sensing Mechanisms for Design of Fluorescent Chemosensors Emerging in Recent Years. *Chem. Soc. Rev.* **2011**, *40*, 3483−3495.

(28) Jason, C. S.; Antonio, G.. D.; Arnold, L. R.; William, C. T. Synthesis, Luminescence Properties, and Explosives Sensing with 1,1-Tetraphenylsilole- and 1,1-Silafluorene-Vinylene Polymers. *Chem. Mater.* **2007**, *19*, 6459−6470.

(29) Davidson, W. R.; Stott, W. R.; Sleeman, R.; Akery, A. K. Synergy or Dichotomy: Vapor and Particle Sampling in the Detection of Contraband. *SPIE* **1994**, *2092*, 108−119.

(30) Kim, T. H.; Lee, B. Y.; Jaworski, J.; Yokoyama, K.; Chung, W.-J.; Wang, E.; Hong, S.; Majumdar, A.; Lee, S.-W. Selective and Sensitive TNT Sensors Using Biomimetic Polydiacetylene-Coated CNT-FETs. *ACS Nano* **2011**, *5*, 2824−2830.

(31) Sanchez, J. C.; Trogler, W. C. Efficient Blue-Emitting Silafluorene−Fluorene-Conjugated Copolymers: Selective Turn-off/Turn-on Detection of Explosives. *J. Mater. Chem.* **2008**, *18*, 3143−3156.

(32) Kartha, K. K.; Babu, S. S.; Srinivasan, S.; Ajayaghosh, A. Attogram Sensing of Trinitrotoluene with a Self-Assembled Molecular Gelator. *J. Am. Chem. Soc.* **2012**, *134*, 4834−4841.